1

Basic Concepts in Distillation

1.1 INTRODUCTION

Distillation is a thermal separation method for separating mixtures of two or more substances into its component fractions of desired purity, based on differences in volatilities of components—which are in fact related to the boiling points of these components—by the application and removal of heat. Note that the term distillation refers to a physical separation process or a unit operation. Remarkably, distillation can be combined with another distillation operation, leading to a dividing-wall column (Harmsen, 2010), or with a chemical reaction, leading to reactive distillation (Sundmacher and Kienle, 2003; Sundmacher, Kienle, and Seidel-Morgenstern, 2005; Luyben and Yu, 2008; Sharma and Singh, 2010), and/or other chemical process operations (Schmidt-Traub and Gorak, 2006).

At the commercial scale, distillation has many applications, such as the separation of crude oil into fractions (e.g., gasoline, diesel, kerosene, etc.), water purification and desalination, the splitting of air into its components (e.g., oxygen, nitrogen, and argon), and the distillation of fermented solutions or the production of distilled beverages with high alcohol content (Forbes, 1970). Distillation underwent enormous development due to the petrochemical industry, and as such it is one of the most important technologies in the global energy supply system (Harmsen, 2010). Essentially, all transportation fuel goes through at least one distillation column on its way from crude oil to readily usable fuel, with tens of thousands of distillation columns in operation worldwide. In view of the foreseen depletion of fossil fuels and the switch to renewable sources of energy such as biomass, the most likely transportation fuel will be ethanol,

Advanced Distillation Technologies: Design, Control and Applications, First Edition.
Anton Alexandru Kiss.

methanol, or derivatives. The synthesis of alternative fuels leads typically to aqueous mixtures that require distillation to separate ethanol or methanol from water. Consequently, distillation remains the separation method of choice in the chemical process industry. The importance of distillation is unquestionable in providing most of the products required by our modern society (e.g., transportation fuel, heat, food, shelter, clothing, etc.).

The analysis, design, operation, control, and optimization of distillation columns were studied extensively in the last century but, until the introduction of computers, only hand calculations and graphical methods were developed and applied in distillation studies. As distillation analysis involves many iterative vapor–liquid phase equilibrium calculations, and tray-to-tray component balances that are ideal for digital computation, the use of computers has had a beneficial effect in recent decades (Luyben, 2011). Many companies still have their own in-house process simulators, although commercial steady-state and dynamic process simulators (e.g., Aspen Plus®, Aspen Dynamics®, ChemCAD, Aspen HYSYS®, PRO/II, etc.) are now available and dominate the field—with distillation playing a key role in these simulators.

The topic of distillation is very broad and it would require many volumes to cover it in a comprehensive manner. Consequently, for more details the reader is directed to several good books, which cover this subject in great detail: Kister (1992a), Kister (1992b), Taylor and Krishna (1993), Stichlmair and Fair (1998), Seader and Henley (1998), Doherty and Malone (2001), Mujtaba (2004), Petlyuk (2004), Lei, Chen, and Ding (2005), and more recently Luyben (2006, 2011).

It is important to note that distillation can separate chemical components only if the compositions of the vapor and liquid phases that are in equilibrium with each other are different. Therefore, a practical understanding of vapor–liquid equilibrium (VLE) is essential for the analysis, design, and control of distillation columns. This introductory chapter presents in a structured and convenient way the basic concepts of distillation: property methods, vapor pressure, bubble point, relative volatility, VLE, vapor–liquid–liquid equilibrium (VLLE), ternary diagrams, residue curve maps (RCM), and theoretical stage and short-cut design methods for distillation.

1.2 PHYSICAL PROPERTY METHODS

An extremely important issue in distillation calculations is the selection of an appropriate physical property method that will accurately describe the phase equilibrium of the chemical system. Missing or inadequate physical properties can undermine the accuracy of a model or even prevent one from performing the simulation. For this reason, finding good values for inadequate or missing physical property parameters is crucial to a successful simulation. Nevertheless, this depends strongly upon choosing the right estimation methods—an issue already recognized in the world of chemical processes modeling by the axiom "garbage in, garbage out" which means that the simulation results have the same quality as the input data/parameters (Carlson, 1996). In most design situations there is some type of data—for example, VLE reported in the literature, experimental measurements, and data books (Gmehling *et al.*, 1993; Perry and Green, 1997)—that can be used to select the most appropriate physical property method. The process simulators used nowadays (e.g., Aspen Plus, ChemCAD, HYSYS, PRO/II) have libraries with numerous alternative methods—the most commonly used being NRTL, UNIQUAC, UNIFAC, Chao–Seader, van Laar, Wilson, Grayson, Peng–Robinson, Soave–Redlich–Kwong (SRK), and derivatives of them.

Figure 1.1 provides a very convenient scheme that can be used for the quick and easy selection of an appropriate property model for virtually any chemical system (Aspen Technology, 2010a, 2010b). The property model names used here are given as in the Aspen Plus process simulator. Table 1.1 summarizes the commonly used property methods available in Aspen Plus (Aspen Technology, 2010b).

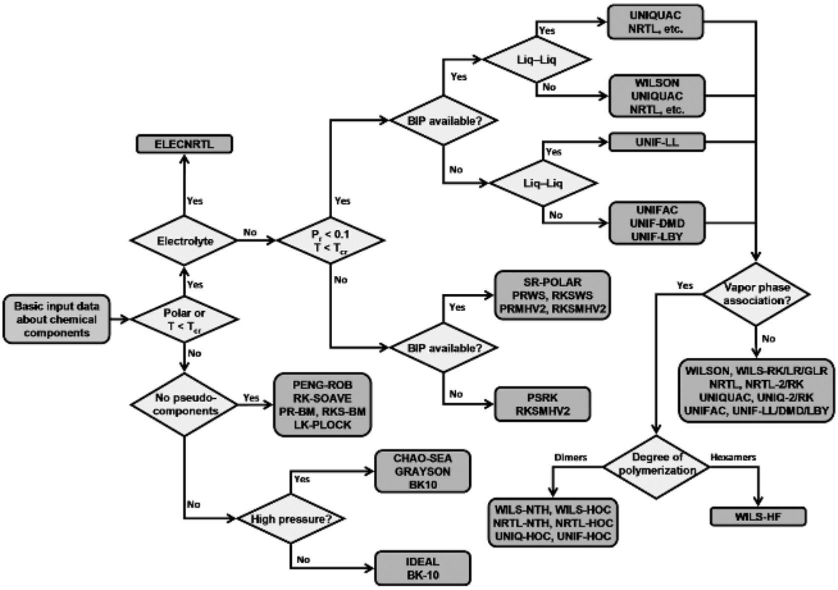

Figure 1.1 Property methods selection scheme

Table 1.1 Summary of commonly used property methods available in Aspen Plus

Abbreviation	*K*-value method	
IDEAL	Ideal gas/Raoult's law/Henry's law	
SOLIDS	Ideal gas/Raoult's law/Henry's law/solid activity coefficients	
BK-10	Braun K-10	
CHAO-SEA	Chao–Seader corresponding states model	
GRAYSON	Grayson–Streed corresponding states model	
STEAM-TA	ASME steam table correlations	
STEAMNBS	NBS/NRC steam table equation of state	
AMINES	Kent–Eisenberg amines model	
APISOUR	API sour water model	
	Equation of state	
BWR-LS	BWR Lee–Starling	
LK-PLOCK	Lee–Kesler–Plöcker	
PENG-ROB	Peng–Robinson	
PR-BM	Peng–Robinson with Boston–Mathias alpha function	
PRWS	Peng–Robinson with Wong–Sandler mixing rules	
PRMHV2	Peng–Robinson with modified Huron–Vidal mixing rules	
PSRK	Predictive Redlich–Kwong–Soave	
RKSWS	Redlich–Kwong–Soave with Wong–Sandler mixing rules	
RKSMHV2	Redlich–Kwong–Soave with modified Huron–Vidal mixing rules	
RK-ASPEN	Redlich–Kwong–ASPEN	
RK-SOAVE	Redlich–Kwong–Soave	
RKS-BM	Redlich–Kwong–Soave with Boston–Mathias alpha function	
SR-POLAR	Schwartzentruber–Renon	
Abbreviation	Liquid activity coefficient	Vapor fugacity coefficient
PITZER	Pitzer	Redlich–Kwong–Soave
PITZ-HG	Pitzer	Redlich–Kwong–Soave

B-PITZER	Bromley–Pitzer	Redlich–Kwong–Soave
ELECNRTL	Electrolyte NRTL	Redlich–Kwong
ENRTL-HF	Electrolyte NRTL	HF hexamerization model
ENRTL-HG	Electrolyte NRTL	Redlich–Kwong
NRTL	NRTL	Ideal gas
NRTL-HOC	NRTL	Hayden–O'Connell
NRTL-NTH	NRTL	Nothnagel
NRTL-RK	NRTL	Redlich–Kwong
NRTL-2	NRTL (using dataset 2)	Ideal gas
UNIFAC	UNIFAC	Redlich–Kwong
UNIF-DMD	Dortmund-modified UNIFAC	Redlich–Kwong–Soave
UNIF-HOC	UNIFAC	Hayden–O'Connell
UNIF-LBY	Lyngby-modified UNIFAC	Ideal gas
UNIF-LL	UNIFAC for liquid–liquid systems	Redlich–Kwong
UNIQUAC	UNIQUAC	Ideal gas
UNIQ-HOC	UNIQUAC	Hayden–O'Connell
UNIQ-NTH	UNIQUAC	Nothnagel
UNIQ-RK	UNIQUAC	Redlich–Kwong
UNIQ-2	UNIQUAC (using dataset 2)	Ideal gas
VANLAAR	Van Laar	Ideal gas
VANL-HOC	Van Laar	Hayden–O'Connell
VANL-NTH	Van Laar	Nothnagel
VANL-RK	Van Laar	Redlich–Kwong
VANL-2	Van Laar (using dataset 2)	Ideal gas
WILSON	Wilson	Ideal gas
WILS-HOC	Wilson	Hayden–O'Connell
WILS-NTH	Wilson	Nothnagel
WILS-RK	Wilson	Redlich–Kwong
WILS-2	Wilson (using dataset 2)	Ideal gas
WILS-HF	Wilson	HF hexamerization model
WILS-LR	Wilson (liquid enthalpy reference state)	Ideal gas
WILS-GLR	Wilson (ideal gas, liquid enthalpy reference state)	Ideal gas
WILS-VOL	Wilson with volume term	Redlich–Kwong

1.3 VAPOR PRESSURE

Distillation is based on the fact that the vapor of a boiling mixture will be richer in the components with lower boiling points. Consequently, when this vapor is sufficiently cooled the condensate will contain more volatile (e.g., light, low-boiling) components, while at the same time the original mixture will contain more of the less volatile (e.g., heavy, high-boiling) components.

Vapor pressure—a physical property of a pure chemical component—is the pressure that a pure component exerts at a given temperature when both liquid and vapor phases are present. In other words, the vapor pressure of a liquid at a particular temperature is the equilibrium pressure exerted by the molecules leaving and entering the liquid surface. Here are some key issues to consider:

- Vapor pressure is related to boiling, and it increases with the energy input.
- A liquid boils when its vapor pressure equals the ambient pressure.
- The ease with which a liquid boils depends on its volatility. Distillation occurs because of the differences in volatility of the components in the liquid mixture.
- Liquids with a high vapor pressure (volatile liquids) boil at low temperatures, and vice versa.
- The vapor pressure (and also the boiling point) of a liquid mixture depends on the relative amounts of the components in the mixture.

Table 1.2 provides the vapor pressure of some common substances at ambient temperature. Note that chemicals with a non-zero vapor

Table 1.2 Vapor pressure of some common substances at 20 °C

Chemical component	Vapor pressure (bar)	Vapor pressure (mmHg)
Ethylene glycol	0.005	3.75
Water	0.023	17.5
Propanol	0.024	18.0
Ethanol	0.058	43.7
Methyl isobutyl ketone (MIBK)	0.265	198.6
Freon 113 (1,1,2-trichlorotrifluoroethane)	0.379	284
Acetaldehyde	0.987	740
Butane	2.2	1650
Formaldehyde	4.357	3268
Carbon dioxide	57	42753

pressure lower than atmospheric are liquids, while those with a vapor pressure higher than atmospheric are gases, under normal conditions.

Raoult's law states that the vapor pressure of an ideal solution is dependent on the vapor pressure of each chemical component and on the mole fraction of the component present in the solution. Once the components in the solution have reached equilibrium, the total vapor pressure (p) of the solution is:

$$p = \sum_{j=1}^{N_C} p_j = \sum_{j=1}^{N_C} p_j^* x_j \tag{1.1}$$

with the individual vapor pressure for each component defined as: $p_j = p_j^* x_j$, where p_j is the partial pressure of component j in the mixture (in the solution), p_j^* is the vapor pressure of the pure component j, and x_j is the mole fraction of component j in the mixture.

The vapor pressure depends only on temperature and not on composition, since it is a pure component property. The dependence on temperature is usually a strong one, with an exponential increase of the vapor pressure at higher temperatures. Figure 1.2a shows some typical vapor pressure curves, for benzene, toluene, and xylene—with the exponential increase clearly observable at high temperatures. Figure 1.2b plots the natural log of the vapor pressure versus the reciprocal of the absolute temperature. It can be seen that as temperature increases (to the left of the plot) the vapor pressure is higher. In both plots of Figure 1.2, a vertical (constant temperature) line shows that, at a given temperature, benzene has a higher vapor pressure than toluene and xylene. Therefore, benzene is the *lightest* component, while xylene is the *heaviest* component—from the volatility (not density) standpoint. Correspondingly, a horizontal (constant-pressure)

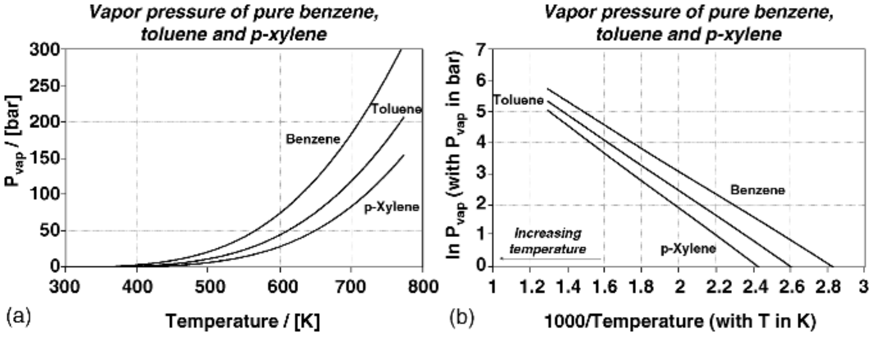

Figure 1.2 Vapor pressure of pure components: benzene, toluene, and p-xylene

line shows that benzene boils at a lower temperature than does toluene or xylene. Therefore, benzene is the *lowest boiling* component, while xylene is the *highest boiling* component. Note also that in Figure 1.2a the vapor pressure lines for benzene, toluene, and xylene are fairly parallel, meaning that the ratio of the vapor pressures does not change much with the temperature or pressure. Consequently, the ease or difficulty of benzene/toluene/xylene separation—directly translated into the energy requirements for the specified separation—does not change much with the operating pressure. However, other chemical components can have temperature dependences of the vapor pressure that are quite different to this example (Luyben, 2006).

In the case of distilling the binary mixture benzene–toluene, the concentration of the lighter (low-boiling) benzene in the vapor phase will be higher than that in the liquid phase—while the reverse is true for the heavier (high-boiling) toluene. As a result, benzene and toluene can be separated in a distillation column into a top distillate stream that is almost pure benzene and a bottoms stream that is fairly pure toluene. Using experimental vapor pressure data for each component, equations can be fitted by means of two, three, or more parameters. The Antoine equation—derived from the Clausius–Clapeyron relation—relates the vapor pressure and temperature for pure components:

$$\log p = A - B/(C + T) \tag{1.2}$$

where p is the vapor pressure, T is temperature, and A, B, and C are constants specific for each pure chemical component—their numerical values depend on the units used for vapor pressure (e.g., bar, mmHg, kPa) and on the units used for temperature (°C or K). The simplified form with the constant C set to zero ($\log p = A - B/T$) is known as the August equation, and describes a linear relation between the logarithm of the pressure and the reciprocal temperature—assuming that the heat of vaporization is independent of temperature.

1.4 VAPOR–LIQUID EQUILIBRIUM AND VLE NON-IDEALITY

1.4.1 Vapor–Liquid Equilibrium

Vapor–liquid equilibrium data for two-component (binary) systems is commonly represented by means of *T–xy* and xy diagrams—where T is the temperature, and x, y are the liquid and vapor composition, respectively, expressed in mole fraction. Basically, the *T*–*xy* diagram plots the temperature versus the liquid and vapor composition, while the *xy* diagram plots only *y* versus *x*. Although these types of diagrams are generated at a constant pressure, the *T*–*xy* an *xy* diagrams are extremely convenient for the analysis of binary distillation systems—especially since the operating pressure is relatively constant in most distillation columns.

Figure 1.3 shows the *T*–*xy* diagram (also known as the boiling point diagram) for the benzene–toluene system at atmospheric pressure—that is, how the equilibrium compositions of the components in a liquid mixture vary with temperature at a fixed pressure. The boiling point of benzene is that at which the mole fraction of benzene is 1, while the boiling point of toluene is that at which the mole fraction of benzene is 0. As illustrated by the *T*–*xy* diagram, benzene is the more volatile component and therefore has a lower boiling point than toluene. The lower curve in the *T*–*xy* diagram is called the *bubble-point curve* (saturated liquid curve), while the upper one is known as the *dew-point curve* (saturated vapor curve). The saturated liquid/lower curve gives the mole fraction of benzene in the liquid phase (*x*) while the saturated vapor/upper curve gives the mole fraction of benzene in the vapor phase (*y*). Drawing a horizontal line at a certain temperature and reading off the intersection of this line with the two curves give the compositions of the two liquid and vapor phases. Note that the *bubble-point* is defined as the temperature at which the liquid starts to boil, while the *dew-point* is the temperature at which the saturated vapor starts to condense. The

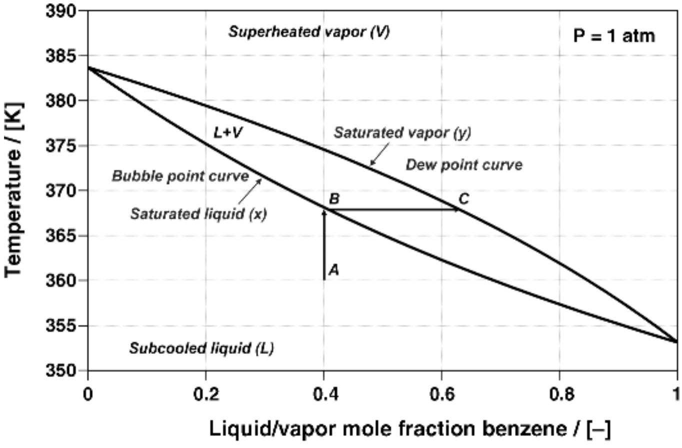

Figure 1.3 *T*–*xy* diagram for the mixture benzene–toluene at atmospheric pressure

region below the bubble-point curve shows the equilibrium composition of the subcooled liquid, while the region above the dew-point curve shows the equilibrium composition of the superheated vapor. Note that in the region between the lower and upper curves, there are two phases present—both liquid and vapor. For example, when a subcooled liquid is heated (point A, at 0.4 mole fraction of benzene) its concentration remains constant until it reaches the bubble-point (point B) when it starts to boil. The vapors produced during the boiling have the equilibrium composition of point C (ca. 0.65 mole fraction of benzene), and are thus over 60% richer in benzene than the original liquid mixture. This difference between the liquid and vapor compositions is in fact the basis for distillation operations.

The *T–xy* diagram can be easily generated in process simulators such as Aspen Plus, and the results at several pressures can be plotted (Figure 1.4). It is important to note that the higher the pressure, the higher the temperatures.

The *xy* diagram is also an effective tool in the analysis of distillation systems. Figure 1.5 illustrates the *xy* diagrams for the binary mixture benzene–toluene (Figure 1.5a) and propane–propylene (Figure 1.5b). As benzene and toluene have a relatively large difference in boiling points, the curve is noticeably shifted from the diagonal ($x = y$). However, propylene and propane have quite close boiling points, which leads to a very difficult separation—as illustrated in the *xy* diagram by the fact that the curve is very close to the diagonal ($x = y$). Remarkably, both *T–xy* and xy diagrams

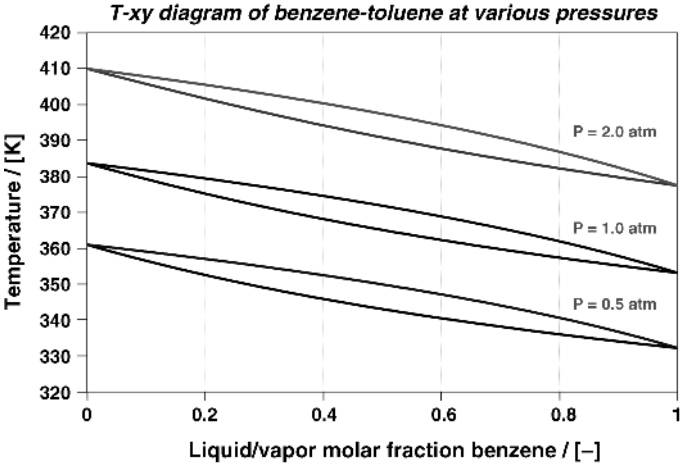

Figure 1.4 *T–xy* diagram for the mixture benzene–toluene at various pressures

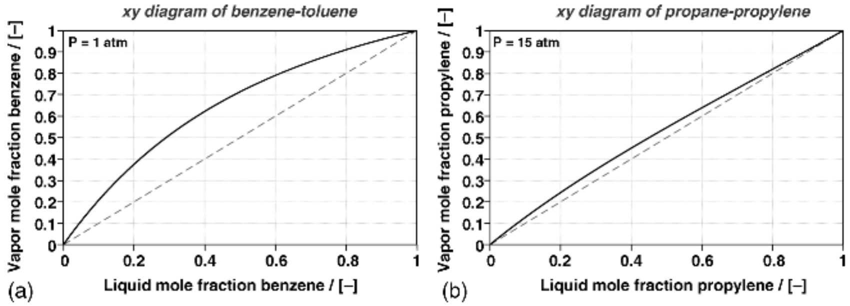

Figure 1.5 The *xy* diagram for the mixture benzene–toluene (a) and propane–propylene (b)

provide valuable insight into the phase equilibrium of binary systems, as they can be used for quantitative analysis of distillation (Luyben, 2006).

1.4.2 VLE Non-ideality

Liquid-phase ideality—equivalent to activity coefficients $\gamma_j = 1$ (unity)—occurs only when the components are very similar. The benzene–toluene system described earlier is a common example, where the activity coefficients of both components are very close to unity. However, if the components are quite different then non-ideal behavior occurs. For example, let us consider a methanol–water mixture; here water is very polar but methanol is polar only at the -OH end of the molecule while the -CH_3 end is non-polar. This difference results in some non-ideality (Figure 1.6). Figure 1.6a gives the *T–xy* curve at atmospheric pressure,

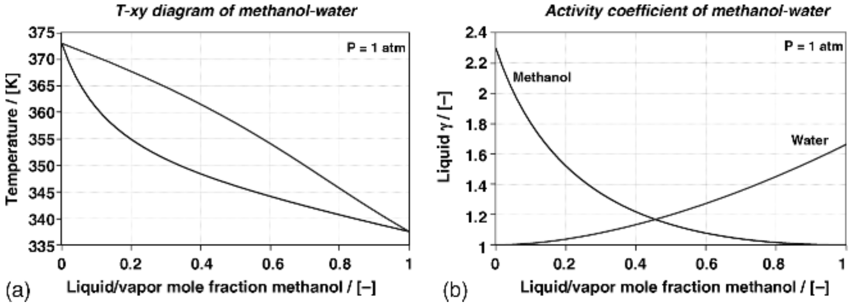

Figure 1.6 *T–xy* diagram (a) and activity coefficient plot (b) for methanol–water

while Figure 1.6b shows the variation of activity coefficients for both water and methanol over the composition space. The NRTL physical property method was used in this example to generate these plots. The activity coefficient values range up to $\gamma = 2.3$ for methanol at the $x = 0$ limit and $\gamma = 1.66$ for water at $x = 1$ (Luyben, 2006).

Let us consider now an ethanol–water mixture, in which case the -CH_2CH_3 (ethyl) end of the ethanol molecule is more non-polar than the -CH_3 end of methanol. As expected, the non-ideality is more pronounced—as clearly illustrated by the *T–xy* and *xy* diagrams shown in Figure 1.7. Note that the *xy* curve shown in Figure 1.7b crosses the diagonal (45° line, where $x = y$) at about 90 mol.% ethanol—this clearly indicates the presence of an azeotrope. Note also that the temperature at the azeotropic composition (351.0 K) is slightly lower than the boiling point of ethanol (351.5 K).

In fact, the most intriguing VLE curves are generated by azeotropic systems that give rise to VLE plots where the equilibrium curves crosses the diagonal (on the *xy* diagram). Note that an azeotrope is defined as the composition at which the liquid and vapor compositions are equal. When this occurs in a distillation column, there is no further change in the liquid and vapor compositions from tray to tray—hence the azeotrope represents a *distillation boundary*. Azeotropes can be classified according to the phase as *homogeneous* (single liquid phase) or *heterogeneous* (two liquid phases), according to the boiling temperature as *minimum-boiling* or *maximum-boiling*, and they can occur in binary, ternary, and multicomponent systems. The ethanol–water mixture described in the previous example has a minimum-boiling homogeneous azeotrope (single liquid phase boiling at 78 °C, with the composition of 89.3 mol.% ethanol). The VLE non-ideality and the types of azeotropic systems are tackled in more detail by Stichlmair and Fair (1998).

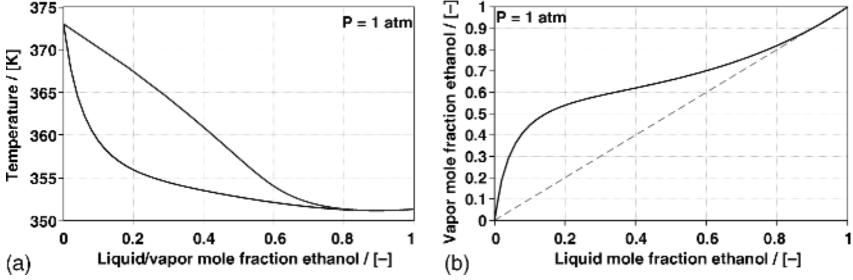

Figure 1.7 *T–xy* diagram, activity coefficient plot (a) and *xy* diagram (b) for ethanol–water

1.5 RELATIVE VOLATILITY

Relative volatility is a measure of the differences in volatility (or boiling points) between two components, indicating how easy or difficult a particular separation will be. The golden rule for distillation is that the larger the relative volatility, the easier the separation. The relative volatility of component L (light) with respect to component H (heavy) is defined as the ratio of the y/x values (vapor mole fraction divided by the liquid mole fraction):

$$\alpha_{\mathrm{LH}} = \frac{y_{\mathrm{L}}/x_{\mathrm{L}}}{y_{\mathrm{H}}/x_{\mathrm{H}}} \tag{1.3}$$

Note that relative volatilities can be applied to both binary and multicomponent systems. In binary systems, the relative volatility α between the light and heavy components can be used to give a simple relationship between the composition of the liquid phase and the vapor phase, with x and y being the mole fraction of the light component in the liquid and vapor phase, respectively:

$$y = \frac{\alpha x}{1 + (\alpha - 1)x} \tag{1.4}$$

Figure 1.8 gives the xy curves for several values of α—under the assumption that α is constant over the entire composition space. For multicomponent systems, a similar relationship can be derived. Consider N_{C}, the number components, with component 1 being the lightest,

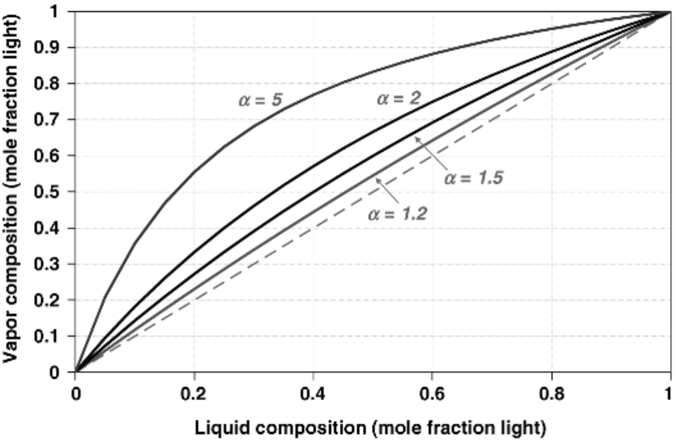

Figure 1.8 The xy curves for various relative volatilities: $\alpha = 1.2$, 1.5, 2, and 5

component 2 is the next lightest, and so forth down to component N_C, the heaviest (H) of all. The relative volatility of component j with respect to component H is defined as (Luyben, 2006):

$$\alpha_j = \frac{y_j/x_j}{y_H/x_H} \tag{1.5}$$

Solving for y_j and summing all the y values, which must add to unity, leads to:

$$y_j = \alpha_j x_j \frac{y_H}{x_H} \tag{1.6}$$

$$\sum_{j=1}^{N_C} y_j = \sum_{j=1}^{N_C} \alpha_j x_j \frac{y_H}{x_H} = \frac{y_H}{x_H} \sum_{j=1}^{N_C} \alpha_j x_j = 1 \tag{1.7}$$

Then, solving for y_H/x_H and substituting this ratio into the first equation above give:

$$\frac{y_H}{x_H} = 1 / \sum_{j=1}^{N_C} \alpha_j x_j \tag{1.8}$$

$$y_j = \alpha_j x_j / \sum_{j=1}^{N_C} \alpha_j x_j \tag{1.9}$$

The last equation relates the vapor composition to the liquid composition for a constant relative volatility multicomponent system. If the relative volatilities are not constant, this equation cannot be used and bubble point calculations are required instead (Luyben, 2006).

1.6 BUBBLE POINT CALCULATIONS

When heating a liquid consisting of two or more components, the bubble point is the temperature at which the first bubble of vapor is formed. Since the vapor will probably have a different composition than that of the liquid, the bubble point—as well as the dew point—at different compositions is very valuable data when designing distillation systems. Note that for single-component mixtures the bubble point and the dew point are the same, and are commonly referred to as the *boiling point*.

The most common VLE problem is to calculate the temperature and vapor composition (y_j) that is in equilibrium with a liquid of known composition (x_j), at a known total pressure (P) of the system. At equilibrium, the *chemical potential* of each component in the liquid and vapor phases are equal:

$$\mu_j^{\mathrm{L}} = \mu_j^{\mathrm{V}} \tag{1.10}$$

The liquid-phase chemical potential of component j can be expressed in terms of liquid mole fraction (x_j), vapor pressure (P_j^{S}), and activity coefficient (γ_j):

$$\mu_j^{\mathrm{L}} = x_j P_j^{\mathrm{S}} \gamma_j \tag{1.11}$$

Similarly, the vapor-phase chemical potential of component j can be expressed in terms of vapor mole fraction (y_j), total system pressure (P), and fugacity coefficient (σ_j):

$$\mu_j^{\mathrm{V}} = y_j P \sigma_j \tag{1.12}$$

Thus, at equilibrium the general relationship between vapor and liquid phases is (Luyben, 2006):

$$y_j P \sigma_j = x_j P_j^{\mathrm{S}} \gamma_j \tag{1.13}$$

The fugacity coefficient is unity ($\sigma_j = 1$) if the total pressure of the system is not too high. Moreover, if the liquid phase is ideal—meaning that there is no interaction between the molecules—then the activity coefficient is unity ($\gamma_j = 1$). However, the occurrence of an ideal liquid phase is much less common than the ideal gas phase, because the components interact in liquid mixtures—they can either attract or repulse (Luyben, 2006). Assuming that both liquid and vapor phases are ideal (i.e., $\sigma_j = 1$ and $\gamma_j = 1$), the bubble point calculation involves an iterative calculation to find the temperature T that satisfies the equation:

$$P = \sum_{j=1}^{N_{\mathrm{C}}} x_j P_{j(T)}^{\mathrm{S}} \tag{1.14}$$

Note that the total pressure P and all x_j values are known, while equations for the vapor pressures of all components as functions of temperature T are also known. Since an analytical derivative of the temperature-dependent vapor pressure functions can be used, the Newton–Raphson convergence method is very convenient and efficient in this iterative calculation (Luyben, 2006).

1.7 TERNARY DIAGRAMS AND RESIDUE CURVE MAPS

Ternary diagrams and reside curve maps are extremely valuable tools for the design of distillation systems, especially when VLE non-ideality is involved (e.g., phase splitting and/or azeotropes).

1.7.1 Ternary Diagrams

Using ternary diagrams, a three-component system can be represented in only two dimensions. Although there are three components, the sum of the mole fractions must add to unity and, as such, specifying two mole fractions is sufficient to define the composition (Luyben, 2006). Figure 1.9a gives a typical rectangular ternary diagram. The mole fraction of component 1 is shown on the abscissa, while the mole fraction of component 2 is shown on the ordinate. Since these axes represent mole fractions, both of these dimensions lie in the interval from zero to one. The three corners of the triangle represent the three pure components, while the edges represent binary mixtures. Any point located within the triangle represents a ternary mixture (Doherty and Malone, 2001; Dimian, 2003; Luyben, 2006).

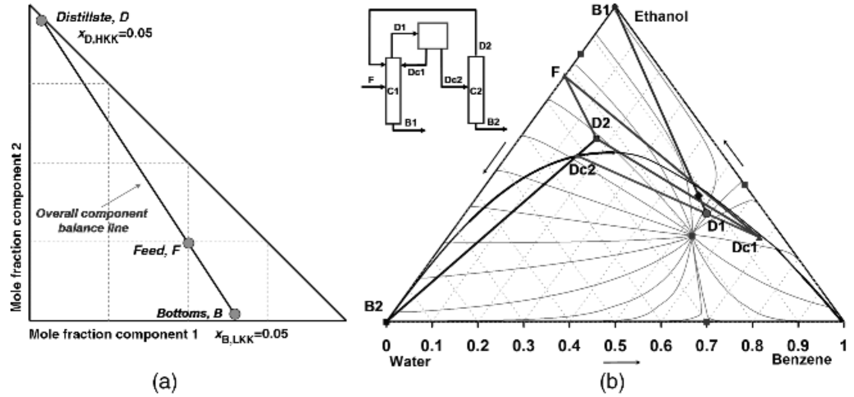

(a) (b)

Figure 1.9 Ternary diagram and mixing rules (a); conceptual design of an azeotropic distillation system: ethanol–benzene–water (b)

Since only two compositions are sufficient to define the composition of a stream, the stream can be easily located on this diagram by entering the appropriate coordinates. For example, Figure 1.9a shows the location of stream *F*, which is a ternary mixture of 50 mol.% component 1, 25 mol.% component 2, and the remaining 25 mol.% is component 3. A useful aspect of ternary diagrams is the *ternary mixing rule,* which states the following. If two ternary streams are mixed together—one being stream *D* (x_{D1}, x_{D2}) and the other stream *B* (x_{B1}, x_{B2})—the mixture has a composition (z_1, z_2) that lies on a straight line in an x_1–x_2 ternary diagram that connects the x_D and x_B points (Luyben, 2006). This property is very useful in separations.

Figure 1.9a also illustrates the application of this mixing rule to a distillation column. Note that instead of mixing, a distillation column separates a feed (*F*) into two product streams (*D* and *B*), but the geometry is exactly the same. The two products *D* and *B* have compositions located at point (x_{D1}, x_{D2}) and (x_{B1}, x_{B2}), respectively. The feed *F* has a composition located at point (z_1, z_2) that lies on a straight line joining *D* and *B*. This geometric relationship is derived from the overall molar balance and the two overall component balances around the column:

$$F = D + B \tag{1.15}$$

$$Fz_1 = Dx_{D1} + Bx_{B1} \tag{1.16}$$

$$Fz_2 = Dx_{D2} + Bx_{B2} \tag{1.17}$$

Substituting the first equation into the second and third gives:

$$(D + B)z_1 = Dx_{D1} + Bx_{B1} \tag{1.18}$$

$$(D + B)z_2 = Dx_{D2} + Bx_{B2} \tag{1.19}$$

Rearranging these two equations to solve for the ratio of *B*/*D* gives:

$$\frac{D}{B} = \frac{z_1 - x_{D1}}{x_{B1} - z_1} \tag{1.20}$$

$$\frac{D}{B} = \frac{z_2 - x_{D2}}{x_{B2} - z_2} \tag{1.21}$$

Equating these two equations and rearranging, results in:

$$\frac{z_1 - x_{D1}}{x_{B1} - z_1} = \frac{z_2 - x_{D2}}{x_{B2} - z_2} \tag{1.22}$$

$$\frac{x_{D1} - z_1}{z_2 - x_{D2}} = \frac{z_1 - x_{B1}}{x_{B2} - z_2} \tag{1.23}$$

This straight-line relationship is very useful in representing what is going on in a ternary distillation system, giving a visual representation of the mass balance of the distillation column. Figure 1.9b demonstrates the use of these rules in a ternary diagram (showing the liquid split envelope) combined with a residue curve map (RCM) for the conceptual design of an azeotropic distillation system: ethanol–benzene–water. The near azeotropic stream F is fed to the first distillation column, together with D2 and Dc1—their mix resides in the triangle F–D2–Dc1. The products of the first column are the bottoms B1 (ethanol) and the distillate D1. The D1 stream is fed to a decanter that separates (according the liquid split tie lines) an organic phase Dc1 (recycled to the first column C1) and an aqueous phase Dc2. The Dc2 stream is fed to a second distillation column C2 that produces the bottoms B2 (water) and a distillate D2 that is recycled to the first column.

1.7.2 Residue Curve Maps

Residue curve maps (RCMs) are a powerful tool for better understanding of the design and operation of distillation columns, especially when the separation involves azeotropic mixtures. Residue curves can be used to determine which separations are possible by distillation. Moreover, compared to stage-to-stage column-composition-profile calculations, residue curves are mathematically much easier to work with and they can provide a great deal of insight into the separation of a mixture. However, despite the current increased computing power, checking the separation feasibility for applications involving mixtures that form two liquid phases is still a relatively complex task. In such heterogeneous systems, RCMs can be used to exploit the two-liquid-phase behavior to facilitate a desired separation. In addition, a RCM can be also used to check the feasibility of separation of homogeneous mixtures and for developing the conceptual design of distillation tower sequences. Separation synthesis based on a RCM enables engineers to develop the best distillation designs, even for complex, highly non-ideal systems that are found in chemical and specialty chemical plants. The ability to visualize the physical constraints of the separation process helps engineers to generate better design alternatives more quickly, resulting in significant time and cost savings.

The simplest form of distillation is a process in which a multicomponent liquid mixture is boiled in an open vessel and the vapor is continuously removed as formed. At any instant in time the vapor is in equilibrium with the remaining liquid. Because the vapor is always richer in the more volatile components than the liquid, the composition of the liquid changes continuously over time, becoming more and more concentrated in the least volatile species. A simple distillation residue curve is a graph showing how the composition of the liquid residue changes over time. A RCM is a collection of liquid residue curves originating from different initial compositions. It contains the same information as phase diagrams, but represented in a more useful way for understanding how to synthesize a distillation sequence. Similarly, for a distillation column equipped with trays, a distillation curve is defined as the locus of the tray compositions at total reflux. A *distillation curve map* (DCM) can be generated easily by choosing a tray liquid composition and stepping up and down by a series of bubble and dew points. Numerical investigation shows that distillation and residue curves are, in general, close to each other. In fact, both are related to the variation of concentration in a distillation column operated at infinite reflux—RCM for a packed column and DCM for a tray column (Doherty and Malone, 2001; Dimian, 2003; Luyben, 2006).

Figure 1.10 shows a typical RCM and the types of characteristic points that can be encountered. All of the residue curves originate at the light (lowest boiling) pure component in a region, move towards the intermediate boiling component, and end at the heavy (highest boiling) pure component in the same region. The lowest temperature nodes are denoted as *unstable nodes* (UNs), as all trajectories leave from them, while the highest temperature points in the region are termed *stable nodes* (SNs), as all trajectories ultimately reach them. The points at which the trajectories approach from one direction and end in a different direction (as always is the point of an intermediate boiling component) are termed *saddle points* (S). Residue curves that divide the composition space into different distillation regions are called distillation boundaries. The concept of characteristic points is important in classifying azeotropic mixtures.

A better understanding of the residue curve map is illustrated in Figure 1.11a. In this example of a zeotropic system, benzene is an unstable

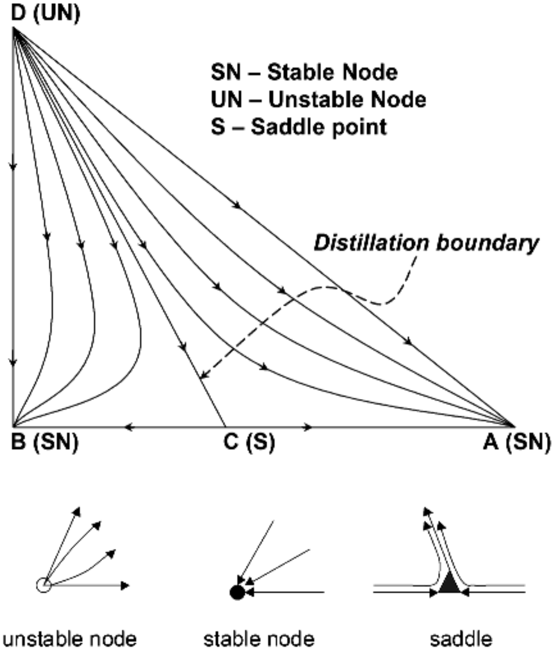

Figure 1.10 Residue curve map (RCM) and types of characteristic points

node, while ethyl-benzene is a stable node and toluene is a saddle point. Note that trajectories move from the lowest temperature towards the highest.

Using various references, the simple distillation process can be described by the set of equations:

$$\frac{\mathrm{d}x_i}{\mathrm{d}\tau} = x_i - y_i; \quad \text{for } i = 1 \ldots n \text{ (number of components)} \tag{1.24}$$

where x_i and y_i are the mole fractions of component i in liquid and vapor phase, respectively, and τ is the nonlinear time scale. Research studies (Stichlmair and Fair, 1998; Doherty and Malone, 2001) have also determined the relationship between the number of nodes (stable and unstable) and saddle points that can exist in a validly drawn RCM. The consistency of RCM with the azeotropic data can be verified by a theoretical test, expressed by the following relation based on topological arguments:

$$4(N_3 - S_3) + 2(N_2 - S_2) + (N_1 - S_1) = 1 \tag{1.25}$$

where N_i and S_i are the number of nodes and saddles, respectively, involving exactly i species from the ternary mixtures. For example, in Figure 1.11a: $N_3 = 0$, $S_3 = 0$, $N_2 = 0$, $S_2 = 1$, $N_1 = 3$, $S_1 = 0$, hence

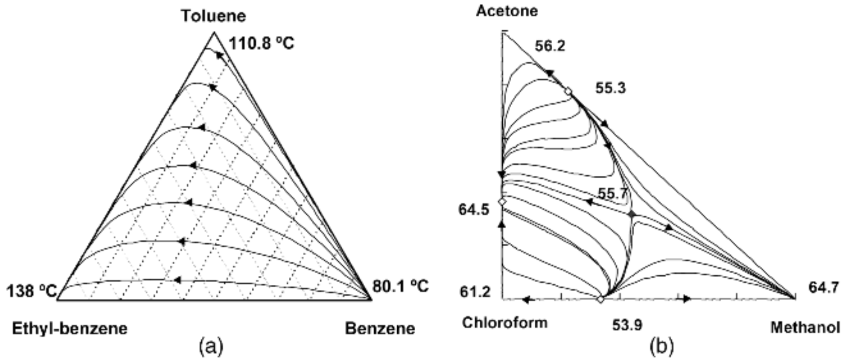

Figure 1.11 RCM for (a) benzene/toluene/ethyl-benzene and (b) acetone/chloroform/methanol

$4(0-0)+2(0-1)+(3-0)=1$. Many different residue curve maps are possible when azeotropes are present (Stichlmair and Fair, 1998; Doherty and Malone, 2001; Petlyuk, 2004).

Residue curve maps have extremely useful applications, such as testing of the consistency of experimental azeotropic data; predicting the order and content of the cuts in batch distillation; checking whether a given mixture is separable by distillation, identification of entrainers, prediction of attainable compositions, and qualitative prediction of composition profile shape; identifying the limiting separation achievable by distillation, and synthesizing separation sequences combining distillation with other methods (Doherty and Malone, 2001; Dimian, 2003; Luyben, 2006).

Note that thermodynamic data is of utmost importance in obtaining reliable RCMs. The adequacy of models and the accuracy of interaction parameters must always be checked. WILSON is very accurate for homogeneous mixtures, while UNIQUAC and NRTL are sufficiently accurate in many cases. An additional advantage is that these models can be applied for both VLE and LLE. Specifying systematically VLLE as an option for flash calculation avoids unreliable azeotrope prediction. UNIFAC should be used only for exploratory purposes, while different sources of equilibrium data should be tested. Nevertheless, when a detailed validated thermodynamic model is not available, pure component and binary azeotropic data often are sufficient to sketch the main characteristics of a RCM. Thereby, it is possible to produce a conceptual design of a separation sequence at an early stage in a project based on very limited information. Notably, nowadays, the generation of a RCM is a standard feature within any process simulator.

Alternatively, a RCM can be represented as a right-angled triangle, a so-called *right-angle triangle diagram,* which is more practical for sketching separation sequences. The following convention is adopted:

A. Pure components: lowest-boiler is on top, intermediate-boiler on bottom-left, and highest-boiler on bottom-right.
B. Azeotropes. A binary azeotrope is represented by a number, which is:
   0: no azeotrope,
   1: binary minimum-boiling azeotrope, node;
   2: binary minimum-boiling azeotrope, saddle;
   3: binary maximum-boiling azeotrope, node;
   4: binary maximum-boiling azeotrope, saddle.
   Ternary azeotrope: m (minimum), M (maximum), or S (intermediate).

For the azeotropic mixture acetone/chloroform/methanol shown in Figure 1.11b the class is 311-S. The first digit represents the maximum-boiling azeotrope acetone/chloroform, the second the minimum-boiling azeotrope chloroform/methanol, the third the minimum-boiling azeotrope acetone/methanol, while the last letter S signifies the ternary saddle azeotrope (Doherty and Malone, 2001; Dimian, 2003).

As explained earlier, all residue curves start at the lightest component and move toward the heaviest component. In this sense they are similar to the compositions in a distillation column. The light components go out the top, and the heavy components go out the bottom. This similarity is very useful for the analysis of distillation systems.

The generation of residue curves can be described mathematically by a dynamic molar balance of the liquid in the vessel M_{liq} and two dynamic component balances for components A and B. The rate of vapor withdrawal (V) is given in moles per unit time:

$$\frac{\mathrm{d}M_{\mathrm{liq}}}{\mathrm{d}t} = -V \tag{1.26}$$

$$\frac{\mathrm{d}(M_{\mathrm{liq}}x_j)}{\mathrm{d}t} = -Vy_j \tag{1.27}$$

The values of x_j and y_j are related by the VLE of the system. Expanding the second equation and substituting the first one gives:

$$M_{\mathrm{liq}}\frac{\mathrm{d}x_j}{\mathrm{d}t} + x_j\frac{\mathrm{d}M_{\mathrm{liq}}}{\mathrm{d}t} = -Vy_j \tag{1.28}$$

$$M_{\text{liq}}\frac{\mathrm{d}x_j}{\mathrm{d}t}+x_j(-V)=-Vy_j \tag{1.29}$$

$$\left(\frac{M_{\text{liq}}}{V}\right)\frac{\mathrm{d}x_j}{\mathrm{d}t}=x_j-y_j \tag{1.30}$$

$$\frac{\mathrm{d}x_j}{\mathrm{d}\theta}=x_j-y_j \tag{1.31}$$

where θ is a dimensionless time variable. The last equation models how the compositions change during the generation of a residue curve. As described next, a similar equation expresses the tray-to-tray liquid compositions in a column under total reflux conditions. This relationship allows the use of residue curves to assess what separations are feasible or infeasible in a given system.

Consider the upper section of a distillation column as shown in Figure 1.12. The column is cut at tray *n,* at which the passing vapor and liquid streams have compositions $y_{n,j}$ and $x_{n+1,j}$, and the flow rates are V_n and L_{n+1}, respectively. The distillate flow rate and composition are

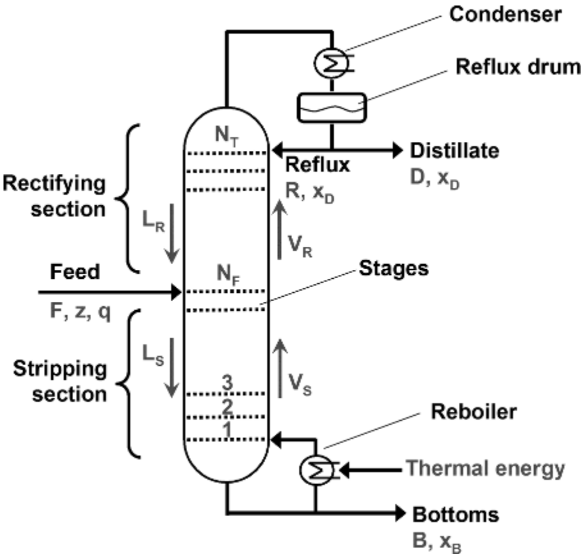

Figure 1.12 Schematics of a distillation column

D and $x_{D,j}$. The steady-state component balance is given by:

$$V_n y_{n,j} = L_{n+1} x_{n+1,j} + D x_{D,j} \tag{1.32}$$

Under total reflux conditions, D is equal to zero and L_{n+1} is equal to V_n. Therefore, $y_{n,j}$ is equal to $x_{n+1,j}$. Now, let us define a continuous variable h as the distance from the top of the column down to any tray. The discrete changes in liquid composition from tray to tray can be approximated by the following differential equation:

$$\frac{\mathrm{d}x_j}{\mathrm{d}h} \approx x_{n,j} - x_{n+1,j} \tag{1.33}$$

At total reflux this equation becomes:

$$\frac{\mathrm{d}x_j}{\mathrm{d}h} = x_{n,j} - y_{n,j} \tag{1.34}$$

Note that this is in fact the same equation as developed for residue curves. The significance of this similarity is that the residue curves approximate the column profiles. Therefore, a feasible separation in a column must satisfy two conditions (Dimian, 2003; Luyben, 2006):

1. The distillate compositions and the bottoms compositions must lie near a residue curve.
2. They must lie on a straight line through the feed composition point.

1.8 ANALYSIS OF DISTILLATION COLUMNS

Figure 1.12 illustrates the schematics of a distillation column consisting of an upper (rectifying) section and a lower (stripping) section, with N_T as the total number of stages. Note that the ideal distillation stage is a device that meets three criteria (Kister, 1992a):

1. It operates in steady state and has a liquid product and a vapor product.
2. All vapor and liquid entering the stage are intimately contacted and perfectly mixed.
3. The total vapor leaving the stage is in equilibrium with the total liquid leaving the stage.

The concept of *stage efficiency* is used to account for the non-ideality of a stage. The number of ideal stages is equal to the number of non-ideal stages multiplied by the stage efficiency. The non-ideality may lower or enhance the separation—if it enhances the separation, the stage efficiency can exceed 100%. Vapor leaving a distillation stage is richer than the feed in the more volatile components. Liquid leaving the stage is richer than the feed in the less volatile components. To improve the separation, multiple stages are used. *Stripping stages* concentrate the less volatile components in a liquid stream. A vapor recycle vaporizes (strips) the more volatile components from the liquid. To generate the vapor recycle to the column, heat is supplied to vaporize a portion of the bottom stage liquid—this vapor recycle is termed as *boil-up*. *Rectifying stages* concentrate the more volatile components in a vapor stream. A liquid recycle condenses the less volatile components from the rising vapor. To generate the liquid recycle, cooling is applied to condense a portion of the overhead vapor—the liquid recycle is termed *reflux*.

The stripping and rectifying stages can be combined into a single separation process with internal recycle (Figure 1.12), termed *distillation* or *fractionation*. In a single feed distillation column, the stages above the feed are rectifying and those below it are stripping. In multi-feed columns, the more precise functional criterion below is used to distinguish the rectifying from stripping sections. The stripping section has a net down flow of material. The vapor serves only as a recycle stream to remove lights from the liquid. Therefore, the quantity of liquid exceeds the quantity of vapor in the stripping section. The converse applies in the rectifying section. This section has a net up flow of material, and the quantity of vapor exceeds the quantity of liquid (Kister, 1992b).

In a multicomponent distillation of j components there are $j-1$ component balances and $j-1$ equations describing the equilibrium relationship. They form the so called MESH equations:

$$\text{Mass balance}: F_n + V_{n+1} + L_{n-1} = V_n + L_n \tag{1.35}$$

$$\text{Component balance}: F_n z_n + V_{n+1} y_{n+1} + L_{n-1} x_{n-1} = V_n y_n + L_n x_n \tag{1.36}$$

Energy balance :

$$\Delta H_n + F_n H_{F,n} + V_{n+1} H_{\mathrm{V},n+1} + L_{n-1} H_{\mathrm{L},n-1} = V_n H_{\mathrm{V},n} + L_n H_{\mathrm{L},n} \tag{1.37}$$

$$\text{Equilibrium relationship}: y_n = K x_n \tag{1.38}$$

These equations apply to each stage. A rigorous solution simultaneously solves these equations for each stage and each component. The equations can be simplified and solved by analytical shortcut procedures or graphically—as described later. The graphical procedures are also applied to introduce and illustrate several key distillation concepts.

1.8.1 Degrees of Freedom Analysis

The design of a distillation column involves many parameters, such as product compositions, product flow rates, operating pressure, total number of trays, feed tray location, reflux ratio (*RR*), reboiler heat input, condenser heat removal, column diameter, and column height. Not all of these variables are independent, so a degrees of freedom (DoF) analysis is useful in pinning down exactly how many independent variables can (and must) be specified to completely define the system. A rigorous DoF analysis involves counting the number of variables in the system and subtracting the number of independent equations that describe the system. For a multicomponent, multistage column this can involve hundreds, if not thousands, of variables and equations. Any error in counting is grossly amplified because we are taking the difference between two very large numbers.

The normal situation in distillation design is that the feed conditions are given: flow rate F (mol h^{-1}), composition z_j (mole fraction of component j), temperature T_F, and pressure P_F. The desired compositions of the product streams are also typically known. Considering a two-product column, the normal specifications are to set the heavy-key impurity in the distillate $x_{D,\mathrm{HK}}$ and the light-key impurity in the bottoms $x_{B,\mathrm{LK}}$. The design problem is to establish the operating pressure P, the total number of trays N_T, and the feed tray location N_F that produces the desired product purities. All the other parameters are then fixed. Therefore, the number of design degrees of freedom is five: $x_{D,\mathrm{HK}}$, $x_{B,\mathrm{LK}}$, P, N_T, and N_F. Consequently, if the desired product purities and the pressure are given there are only two degrees of freedom: N_T and N_F. To emphasize this point, the five variables that could be specified might be the distillate flow rate D, reflux ratio $RR = R/D$, P, N_T, and N_F. In this case the product compositions cannot be specified but depend on the distillate flow rate and reflux ratio selected (Luyben, 2006). The next sections provide some of the ways used to establish reasonable values of some of the parameters such as the number of stages or the reflux ratio.

1.8.2 McCabe–Thiele Method

The McCabe–Thiele method is a graphical approach that shows very nicely in a graphical form the effects of VLE, reflux ratio, and number of trays (McCabe, Smith, and Harriot, 2005). Although it is limited to binary systems, the effects of parameters can be extended to multicomponent systems. The basic effects can be summarized as follows:

- The easier the separation, the fewer trays are required and the lower the required reflux ratio (also translated into lower energy requirements).
- The higher the desired product purities, the more trays are required—but the required reflux ratio does not increase significantly as the product purities increase.
- There is an engineering trade-off between the number of trays and the reflux ratio. An infinite number of columns can be designed that produce exactly the same products but have different heights, diameters, and energy requirements. Hence, selecting the optimum column involves issues of both steady-state economics and dynamic controllability.
- The minimum values of the number of trays (N_{min}) and of the reflux ratio (RR_{min}) required for a given separation.

All of these items can be visually demonstrated using the McCabe–Thiele method. The distillation column considered is shown in Figure 1.12, with the various flows and composition indicated. Assuming that the feed molar flow rate F and composition z are given, if the product compositions are specified, the molar flow rates of the two products D and B can be immediately calculated from the overall total molar balance and the overall component balance on the light component:

$$F = D + B \tag{1.39}$$

$$Fz = Dx_D + Bx_B \tag{1.40}$$

$$D = F\left(\frac{z - x_B}{x_D - x_B}\right) \tag{1.41}$$

For the moment let us assume that the pressure has been specified, so the VLE is fixed. Let us also assume that the reflux ratio has been specified, so the reflux flow rate can be calculated $R = RRD$. The equimolar overflow assumption is usually made in the McCabe–Thiele method. The liquid and vapor flow rates are assumed to be constant in a given section of the column. For example, the liquid flow rate in the rectifying section L_{R} is equal to the reflux flow rate R. From an overall balance around the top of the column, the vapor flow rate in the rectifying section V_{R} is equal to the reflux plus the distillate ($V_{\mathrm{R}} = R + D$). This method uses a *xy* diagram whose coordinates are the mole fraction of the light component in the liquid x and the mole fraction of the light component in the vapor phase y. The diagonal (45° line) is plotted and so is the VLE curve for the selected pressure. The specified product compositions x_D and x_B are located on the diagonal, as described next.

Figure 1.13 illustrates the construction of the rectifying operating line (ROL), while Figure 1.14 shows the construction of the stripping operating line (SOL). The ROL is a straight line with a slope equal to the ratio of the liquid and vapor flow rates in the rectifying section:

$$\text{Slope ROL} = \frac{L_{\mathrm{R}}}{V_{\mathrm{R}}} = \frac{R}{R+D} = \frac{RR}{1+RR} \tag{1.42}$$

The line intersects the diagonal at the distillate composition x_D, and so it is easy to construct—as shown in Figure 1.15. The proof of this ROL construction can be derived by looking at the top of the column, as shown in Figure 1.13 (Luyben, 2006).

The liquid and vapor flow rates in the stripping section (L_{S} and V_{S}) can be calculated if the thermal condition of the feed is known. Since the temperature, pressure, and composition of the feed are given, the fraction of the feed that is liquid—defined as the variable q—can be calculated

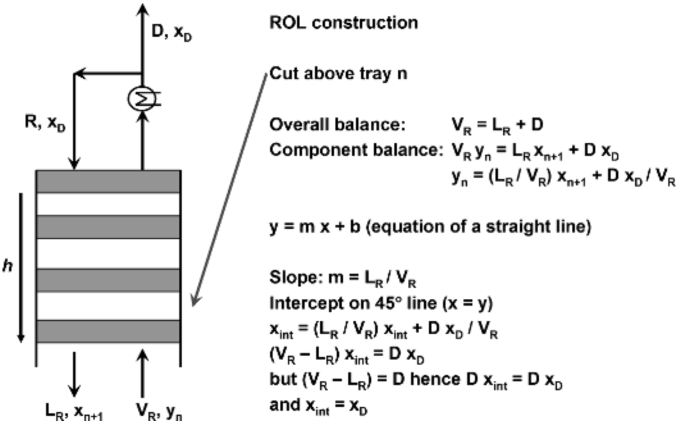

Figure 1.13 Construction of a rectifying operating line (ROL)

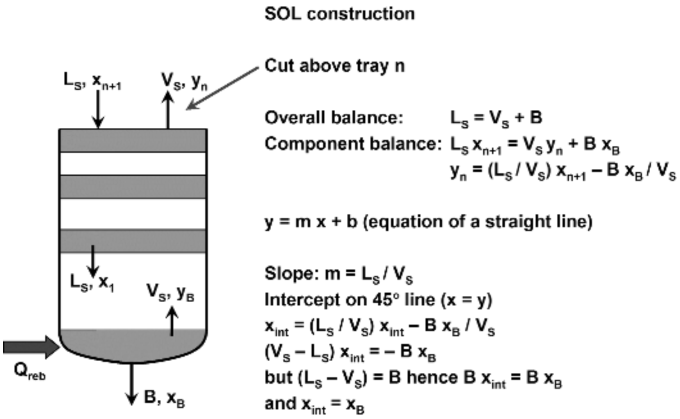

Figure 1.14 Construction of a stripping operating line (SOL)

from an isothermal flash calculation. Knowing q, the liquid and vapor flow rates in the stripping section can be calculated. If the feed is saturated liquid, $q = 1$ and if the feed is saturated vapor, $q = 0$:

$$q = \frac{L_S - L_R}{F} \tag{1.43}$$

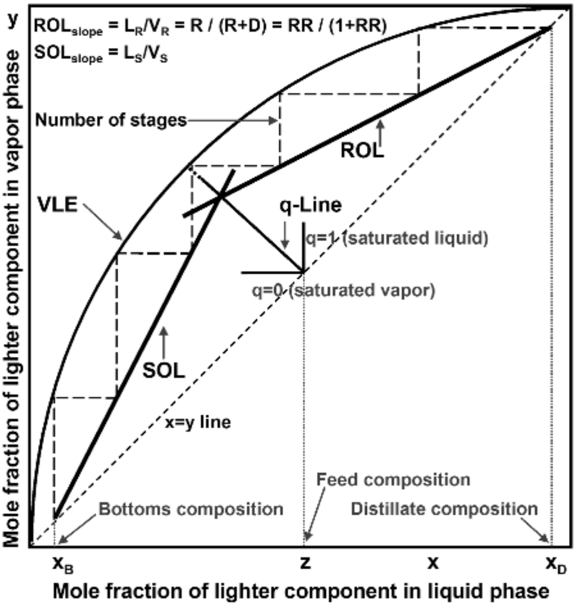

Figure 1.15 McCabe–Thiele method—operating lines and number of stages

$$L_S = qF + L_R \tag{1.44}$$

$$V_S = L_S - B \tag{1.45}$$

The SOL is a straight line with slope L_S/V_S that intersects the diagonal at the bottoms composition x_B. Proof of this construction can be derived by looking at the bottom of the column, as shown in Figure 1.14 (Luyben, 2006). Figure 1.15 shows both operating lines: ROL and SOL. Note that there is a relationship between the intersection point of the two operating lines and feed conditions. As shown in Figure 1.15, a straight line can be drawn from the location of the feed composition z on the diagonal to this intersection point. As proven hereafter, the slope of this line (known as the *q-line*) is a function of only the thermal condition of the feed—defined by parameter q. The slope is $-q/(1-q)$, which makes the construction of the McCabe–Thiele diagram very simple:

- Locate the three compositions on the diagonal (45° line): z, x_D, x_B;
- draw the ROL from the x_D point with a slope of $RR/(1+RR)$;
- draw the q-line from the z point with a slope of $-q/(1-q)$;
- draw the SOL from the x_B point to the intersection of the q-line and the ROL.

The equations of the rectifying and stripping operating lines are given below in terms of the point of intersection of the two lines at y_{int} and x_{int}:

$$\text{ROL}: \quad y_{\text{int}} = \left(\frac{L_R}{V_R}\right)x_{\text{int}} + \frac{Dx_D}{V_R} \tag{1.46}$$

$$\text{SOL}: \quad y_{\text{int}} = \left(\frac{L_S}{V_S}\right)x_{\text{int}} - \frac{Bx_B}{V_S} \tag{1.47}$$

Subtracting the two equations gives:

$$(V_R - V_S)y_{\text{int}} = (L_R - L_S)x_{\text{int}} + (Dx_D + Bx_B) \tag{1.48}$$

The last term on the right-hand side is actually $Fz = Dx_D + Bx_B$. Using the definition of $q = (L_S - L_R)/F$ leads to:

$$(V_R - V_S) = (1 - q)F \tag{1.49}$$

$$(L_R - L_S) = -qF \tag{1.50}$$

Substituting these relationships into the previous equation gives:

$$(1 - q)Fy_{\text{int}} = -qFx_{\text{int}} + Fz \tag{1.51}$$

$$y_{\text{int}} = \left(\frac{-q}{1-q}\right)x_{\text{int}} + \left(\frac{z}{1-q}\right) \tag{1.52}$$

This is in fact the equation of a straight line, with the slope $-q/(1-q)$. The q line is vertical for saturated liquid feed ($q = 1$), and it is horizontal for saturated vapor feed ($q = 0$). On the diagonal, this holds true: $x_{\text{int}} = y_{\text{int}}$. Consequently, it can be demonstrated that the q line intersects the diagonal (45° line) at the feed composition z:

$$(1 - q)x_{45} = -qx_{45} + z \tag{1.53}$$

$$x_{45} = z \tag{1.54}$$

The number of trays is determined by moving vertically from the x_B point on the diagonal to the VLE line—this is in fact the composition of the vapor y_B leaving the partial reboiler. Moving horizontally over to the SOL, this step represents the partial reboiler. The value of x on the SOL is the composition of liquid x_1 leaving tray 1 (when numbering from the bottom of the column up). This stepping is repeated, moving vertically to y_1 and horizontally to x_2. Stepping continues until the intersection of the operating lines is crossed—this is the feed tray. The horizontal line is extended then to the ROL. Continuing to step until the x_D value is crossed gives the total number of trays.

The minimum number of trays for a specified separation corresponds to total reflux operation. If the column is run under total reflux conditions, the distillate flow rate is zero. Therefore, the reflux ratio is infinite, and the slope of the operating lines is unity—this is the 45° line. Thus the minimum number of trays can be determined by simply stepping up between the diagonal (45° line) and the VLE curve, as illustrated in Figure 1.16. The minimum reflux ratio for a specified separation corresponds to having an infinite number of trays. This usually occurs when the operating lines and the q-line intersect exactly on the VLE curve—this is a *pinch condition,* as it would take an infinite number of trays to move past this point. This is also illustrated in Figure 1.16. The minimum reflux ratio is calculated from the slope of this limiting

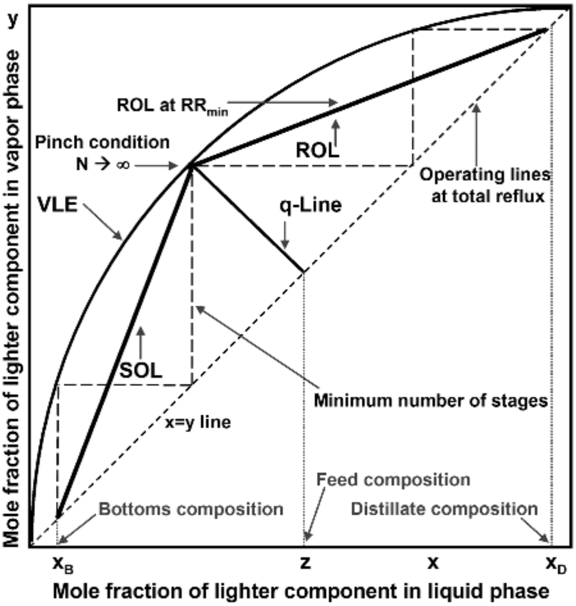

Figure 1.16 McCabe–Thiele method—minimum reflux and minimum number of stages

operating line. The McCabe–Thiele method can be conveniently tested online at: http://www.cheric.org/education/eduaids/distill/McCabe.html (last accessed on 24 December 2012).

Based on the McCabe–Thiele diagram, several observations can be made—which can be applied to all types of separations and distillation columns, not just a binary distillation:

- The further the VLE curve is from the diagonal, the smaller the slope of the rectifying operation line (ROL), meaning a smaller reflux ratio and thus lower energy requirements. A large VLE curve corresponds to large relative volatilities and an easy separation.
- The easier the separation, the fewer trays it takes to make a given separation.
- The higher the product purities, the more trays it takes to make a given separation.
- Increasing product purities does not have a significant effect on the required reflux ratio.
- Increasing the liquid to vapor ratio in a section of a column increases the separation that occurs in that section.

1.8.3 Approximate Multicomponent Methods

Several simple approximate methods were developed for analyzing multicomponent systems, long before the availability of computers for rigorous analysis—the best known being the Fenske–Underwood–Gilliland (FUG) shortcut method. These methods are still quite useful for getting quick estimates of the size of a column (number of trays) and the energy requirements (e.g., reflux ratios and the corresponding vapor boil-up and reboiler heat input):

Fenske equation for minimum number of trays: The minimum number of trays corresponds to total reflux operation (an infinite reflux ratio). The Fenske equation relates the compositions at the two ends of a column to the number of stages in the column under this limiting condition:

$$N_{\min} + 1 = \frac{\log\left[\left(\frac{x_{D,\mathrm{LK}}}{x_{D,\mathrm{HK}}}\right)\left(\frac{x_{B,\mathrm{HK}}}{x_{B,\mathrm{LK}}}\right)\right]}{\log\left(\alpha_{\mathrm{LK,HK}}\right)} \tag{1.55}$$

where $N_{\min}$ is the minimum number of stages required, $x_{D,\mathrm{LK}}$ is the mole fraction of the light-key (LK) component at the top of the column, $x_{D,\mathrm{HK}}$ is the mole fraction of the heavy-key (HK) component at the top of the column, $x_{D,\mathrm{HK}}$ is the mole fraction of the heavy-key component at the bottom of the column, $x_{B,\mathrm{LK}}$ is the mole fraction of the light-key component at the bottom of the column, and $\alpha_{\mathrm{LK,HK}}$ is the relative volatility between the LK and HK components. This equation is applicable to multicomponent systems, but it assumes a constant relative volatility between the two components considered.

Underwood equations for minimum reflux ratio: The Underwood equations can be used to calculate the minimum reflux ratio in a multicomponent system if the relative volatilities of the components are constant. The equations are as follows:

$$\sum_{j=1}^{N_C} \frac{\alpha_j z_j}{\alpha_j - \theta} = 1 - q \tag{1.56}$$

$$\sum_{j=1}^{N_C} \frac{\alpha_j x_{D,j}}{\alpha_j - \theta} = 1 + RR_{\min} \tag{1.57}$$

The following variables are specified: feed composition z_j (mole fractions $j = 1, \ldots N_C$), the desired distillate composition $x_{D,j}$ ($j = 1, \ldots N_C$), and the feed thermal condition q. The relative volatilities α_j ($j = 1, \ldots N_C$) of the multicomponent mixture are known from the VLE. The first equation contains one unknown parameter θ. However, expanding the summation of N_C terms and multiplying through by all the denominator terms $(\alpha_j - \theta)$ gives a polynomial in θ whose order is N_C, which means that there are N_C roots of this polynomial. One of these roots lies between the two relative volatility values α_{LK} and α_{HK}. This is found using some iterative solution method. It is substituted into the second equation, which can then be solved explicitly for the minimum reflux ratio.

Gilliland correlation. An empirical correlation can be used to calculate the final number of stages N from the values calculated through the Fenske and Underwood equations (N_{min}, RR, RR_{min}). Gilliland noted that he could empirically relate the number of stages (N) at a finite reflux ratio (RR) to the minimum number of stages (N_{min}) and the minimum reflux ratio (RR_{min}). The procedure uses a diagram plotting $(RR - RR_{min})/(RR + 1)$ on the x-axis and $(N - N_{min})/(N + 1)$ on the y-axis. One enters the diagram with the abscissa value, which is known, and then it reads the ordinate of the corresponding point on the Gilliland curve. The only unknown of the ordinate is the total number of stages (N).

Kirkbride equation. This is an empirical equation used to determine the number of stages in the rectifying (N_R) and stripping (N_S) sections, and therefore the feed stage location:

$$\frac{N_R}{N_S} = \left[\left(\frac{x_{F,HK}}{x_{F,LK}} \right) \left(\frac{x_{B,LK}}{x_{D,HK}} \right)^2 \frac{B}{D} \right]^{0.206} \tag{1.58}$$

1.9 CONCLUDING REMARKS

The basics of the vapor–liquid phase equilibrium (VLE) reviewed here play a key role, as a very good understanding of VLE is indispensable in the design and control of any distillation system. Most of the key concepts are used extensively throughout this book. Moreover, several practical methods for analyzing distillation columns have been presented. Graphical methods provide valuable insight into how various design and operating parameters affect separations in distillation, while the residue curve map (RCM) representation allows the designer to identify the feasible separations.

REFERENCES

Aspen Technology (2010a) Aspen Plus: User Guide - Volume 1 & 2.

Aspen Technology (2010b) Aspen Physical Property System - Physical Property Models.

Carlson, E.C. (1996) Don't gamble with physical properties for simulations. *Chemical Engineering Progress*, 35–46.

Dimian, A.C. (2003) *Integrated Design and Simulation of Chemical Processes*, Elsevier, Amsterdam.

Doherty, M.F. and Malone, M.F. (2001) *Conceptual Design of Distillation Systems*, McGraw-Hill, New York.

Forbes, R.J. (1970) *A Short History of the Art of Distillation*, E. J. Brill, Leiden.

Gmehling, J., Onken, U., Arlt, W. *et al.* (1993) *Vapor-Liquid Equilibrium Data Collection*, DECHEMA, Frankfurt/Main.

Harmsen, G.J. (2010) Process intensification in the petrochemicals industry: Drivers and hurdles for commercial implementation. *Chemical Engineering and Processing*, ***49***, 70–73.

Kister, H.Z. (1992a) *Distillation – Design*, McGraw-Hill, New York.

Kister, H.Z. (1992b) *Distillation – Operation*, McGraw-Hill, New York.

Lei, Z., Chen, B., and Ding, Z. (2005) *Special Distillation Processes*, Elsevier, Amsterdam.

Luyben, W.L. (2006) *Distillation Design and Control using Aspen Simulation*, John Wiley & Sons, Inc., Hoboken.

Luyben, W.L. (2011) *Principles and Case Studies of Simultaneous Design*, John Wiley & Sons, Inc., Hoboken.

Luyben, W.L. and Yu, C.C. (2008) *Reactive Distillation Design and Control*, John Wiley & Sons, Inc., Hoboken.

McCabe, W.L., Smith, J.C., and Harriot, P. (2005) *Unit Operations of Chemical Engineering*, McGraw-Hill, New York.

Mujtaba, I.M. (2004) *Batch Distillation – Design and Operation*, Imperial College Press, London.

Perry, R.H. and Green, D.W. (eds) (1997) *Perry's Chemical Engineers' Handbook*, McGraw-Hill, New York.

Petlyuk, F.B. (2004) *Distillation Theory and its Application to Optimal Design of Separation Units*, Cambridge University Press, Cambridge.

Schmidt-Traub, H. and Gorak, A. (2006) *Integrated Reaction and Separation Operations*, Springer, New York.

Seader, J.D. and Henley, E.J. (1998) *Separation Process Principles*, John Wiley & Sons, Inc., New York.

Sharma, N. and Singh, K. (2010) Control of reactive distillation column - A review. *International Journal of Chemical Reactor Engineering*, *8*, R5.

Stichlmair, J.G. and Fair, J.R. (1998) *Distillation - Principles and Practice*, Wiley-VCH Verlag GmbH, Weinheim.

Sundmacher, K. and Kienle, A. (eds) (2003) *Reactive Distillation: Status and Future Directions*, Wiley-VCH Verlag GmbH, Weinheim.

Sundmacher, K., Kienle, A., and Seidel-Morgenstern, A. (eds) (2005) *Integrated Chemical Processes: Synthesis, Operation, Analysis, and Control*, Wiley-VCH Verlag GmbH, Weinheim.

Taylor, R. and Krishna, R. (1993) *Multi-component Mass Transfer*, John Wiley & Sons, Inc., New York.